ATOMIZED FUEL JET AND DROPLETS IN THE ENVELOPE STRUCTURE FORMED

Marius Constantin BENIUGA[1], Robert-Adrian CHIȚAN [1], Ioan MIHAI [1]

[1]*Department of Mechanical Engineering, Stefan cel Mare University of Suceava, Romania*
13 University Street, 720229,
e.mail: beniugamarius@gmail.com

Abstract: *This paper studies the peculiarities of fuel jet atomization in multipoint injection systems and will determine the forward and deformation resistance of liquid droplets. It is necessary to determine the drag coefficient of the droplets as a function of the ratio of fuel to air viscosity. Since a dependence of the coefficient of friction on the Reynolds number has been established, it is considered appropriate to analyse the conditions that precede droplet break-up. To this end, a comparative study of droplet shape is carried out.*

Keywords: *atomisation, droplets, airflow.*

1. Introduction

The simulation of the atomisation process aims to validate the results obtained with the analytical models.

For the simulations, known parameters from the experiments are used as input data. Examples are the angle θ of the droplet jet or the jet break-up constant C_λ where the values adopted depend on the injector and the characteristics of the injection system. The way in which the droplets are sprayed is also taken into account: with or without vaporisation, in a controlled isobaric or isochoric environment. Studies on fuel atomisation phenomena in relation to injector wear are extremely rare according to the literature used in the literature.

1.1. Fuel jet parameters

In figure 1 the following parameters are shown: L_b - the depletion length, S - the jet penetration length, θ - the jet deflection angle, SMD - Souter Mean Diameter.

These are taken into account, as they influence the jet breakup.

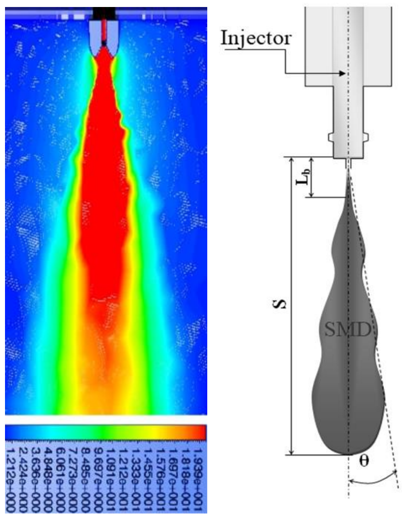

Figure 1. *Fuel jet and its parameters.*

1.2. The drag coefficient of liquid droplets, simulation of their dynamics

A theoretical prediction of the drag coefficient for R_e<1 is given by Taylor and Acrivos [1], shown in equation (1).

$$C_D = \frac{8}{R_e}\frac{2+3\mu_r}{1+\mu_r}\left(1+\frac{R_e}{16}\frac{2+3\mu_r}{1+\mu_r}+\frac{1}{40}\left(\frac{3\mu_r+2}{\mu_r+1}\right)^2\left(\frac{R_e}{2}\right)^2 ln\frac{R_e}{2}\right). \quad (1)$$

For $\mu_r \to \infty$, the drag coefficient will be:

$$C_D = \frac{24}{\mathrm{R}_e}\,. \qquad (2)$$

For $\mu_r \to 0$, the drag coefficient will be:

$$C_D = \frac{16}{\mathrm{R}_e}\,. \qquad (3)$$

Figure 2 simulates the process of breaking up the liquid jet into droplets [2].

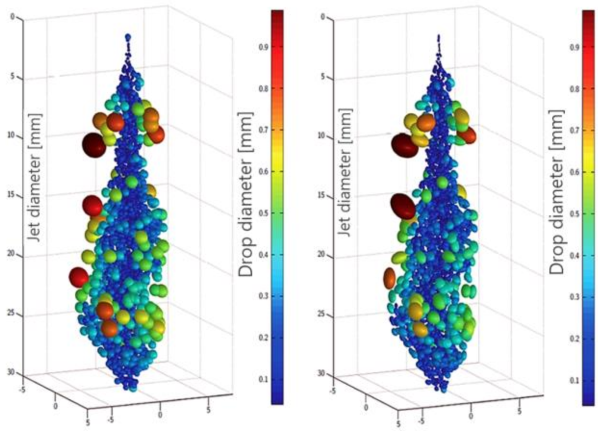

Figure 2. *Simulation of the liquid jet atomization process, [2].*

2. Change in friction coefficient of droplets with the gaseous medium as a function of Reynolds number

For a liquid droplet moving in any gaseous medium, the forces due to aerodynamic resistance to displacement can be determined by knowing the aerodynamic drag coefficient and the cross-sectional area of flow normal to the liquid flow.

In turn the cross-sectional area can be calculated based on the maximum droplet diameter for various assumptions that take into account the shape of the droplets.

It has been found that towards the end of the atomisation process acceleration differences for different droplet sizes lead to small variations in the mean droplet diameter, a phenomenon explained by the "convective mixing" effect.

The shape of droplets moving in a gaseous medium is constantly changing.

Figure 3. shows the results obtained by [3] showing how droplet shape evolves over time.

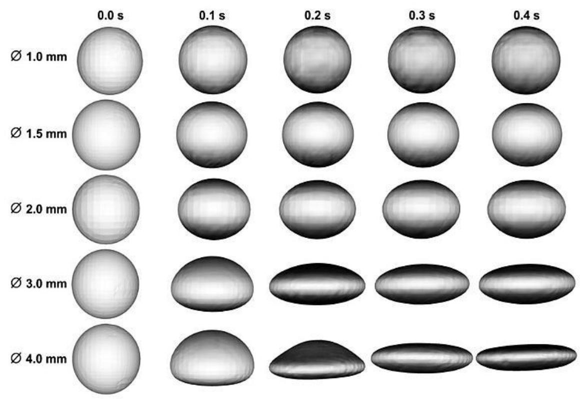

Figure 3. *Deformation of droplets over time for different diameters, [2].*

The images in Figure 3 were obtained for the case where the droplet starts to move from the resting state. It can be seen that the deformation is more pronounced as the diameter of the droplet increases. For droplets with a diameter of 3 [mm] or 4 [mm], the evolution from spherical to spheroid and disc shape is observed.

For each of the three cases, mathematical models have been developed to determine the friction coefficient. Although the present case analyses relatively large droplets, it is not excluded that for droplets of much smaller diameters, moving at high velocities in a gaseous medium leads to similar deformations.

2.1. Calculation for the spherical drop case

The calculation of the friction coefficient was performed using a calculation code [5] developed in Mathcad [7].

Considering the sprayed droplet in the shape of a sphere, the friction coefficient C_{f1} was calculated with the relation deduced by Clift and co-workers, [4] which has the following form:

$$C_{f1} = \frac{24}{R_e}\left(1+0{,}15R_e^{0{,}687}\right) + \frac{0{,}42}{1+4{,}25R_e^{-1{,}16}10^4}\,. \qquad (4)$$

2.2. Calculation for the disc-shaped drop case

For disc-shaped liquid droplets, the friction coefficient C_{f2} is deduced by Clift and co-workers [4] with the relation:

$$C_{f2} = \frac{64}{\pi R_e}\left(1 + 0{,}138 R_e^{0{,}792}\right). \quad (5)$$

where: $R_e \in (1{,}5 \div 133)$.

2.3. Calculation for the spheroid drop case

For spheroid-shaped liquid droplets, Clift and co-workers [4, 6] established for the coefficient of friction, the relationship shown below:

$$C_{f3} = 108{,}42 R_e^{\left[-1{,}66 + 0{,}3958 log(Re) - 0.03 log^2(Re)\right]}. \quad (6)$$

where: $R_e \in (40 \div 104)$.

3. Results obtained for the three forms of the drop

3.2. Results for spherical droplets

Figure 4 shows the values of the calculations performed for the friction coefficient C_{f1} at Reynolds number values Re< 3·105.

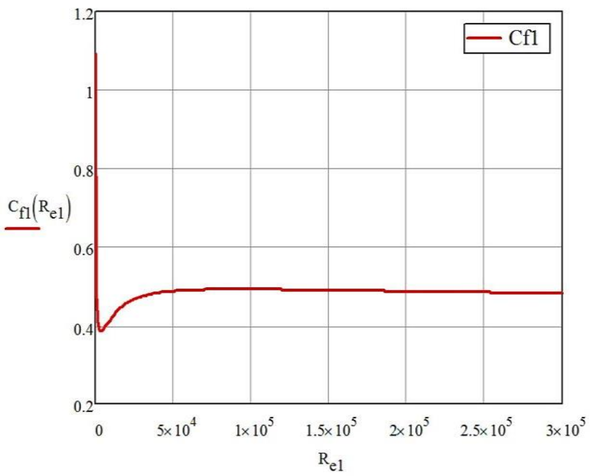

Figure 4. *Friction coefficient as a function of Reynolds number for the spherical droplet.*

3.2. Results obtained for disc-shaped drops

The data obtained using the code for the mathematical model for calculating the coefficient of friction C_{f2} [5], as a function of Reynolds number, allowed Figure 5 to be obtained.

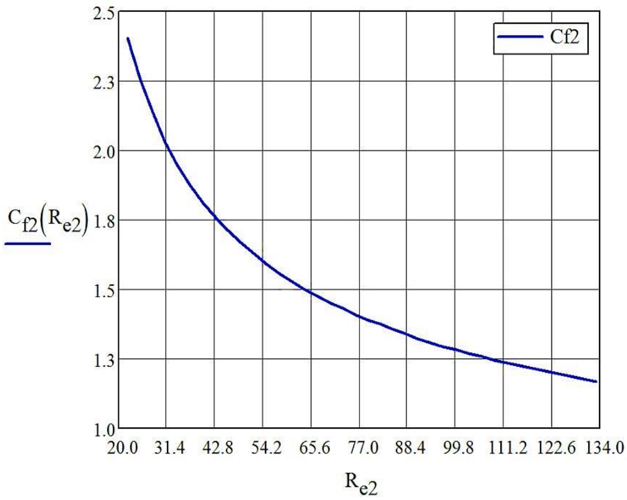

Figure 5. *Friction coefficient as a function of the Reynolds number of the disc-shaped droplet.*

3.3. Results obtained for spheroid droplets

Using the calculation code for determining the friction coefficient C_{f3} as a function of the Reynolds number mentioned [5], Figure 6 was obtained for the spheroid-shaped droplet.

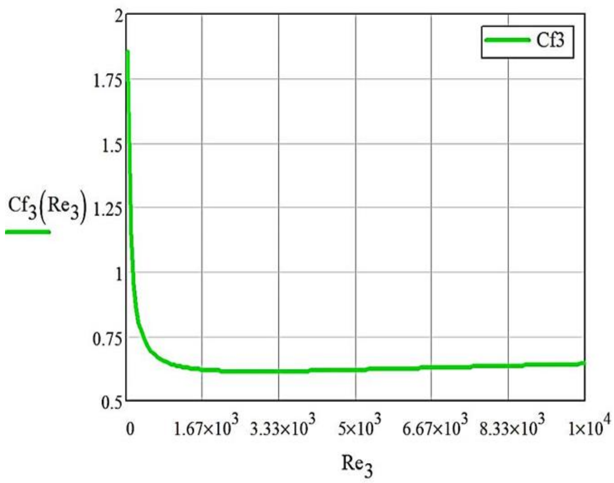

Figure 6. *Friction coefficient of the spheroid droplet as a function of R_e number.*

It is found that there is a range of Reynolds number values for which the friction coefficient increases or decreases very much, marked in Figure 7 by the dashed circles. The results obtained for the aerodynamic friction coefficients corresponding to the spherical and disc-shaped droplets, respectively, as a function of Reynolds number, show much higher values for the first category.

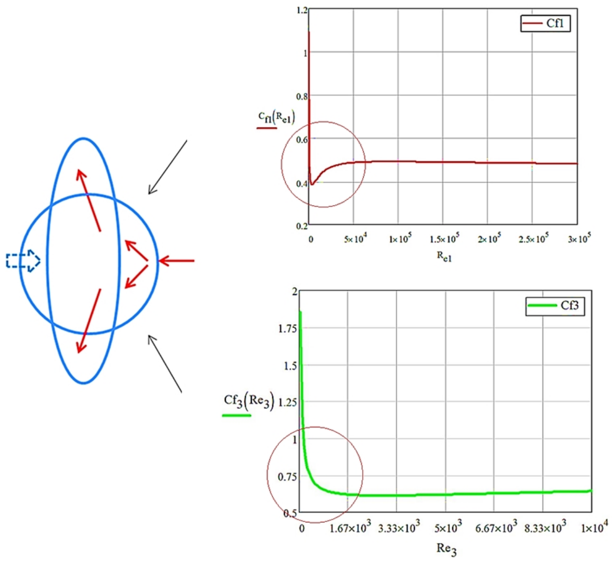

Figure 7. *Friction coefficient of the spheroid droplet as a function of R_e number.*

5. Conclusions

The variation of friction coefficients as a function of Reynolds number, for spherical, disc and spheroid shaped droplets, obtained using equations (4), (5) and (6), undoubtedly show differences in values and modes of evolution characteristic of each case. This is due to the fact that in sphere-shaped droplets the friction coefficient increases with increasing Reynolds number Re due to the larger characteristic size of the shape considered. In disc or spheroid droplets, even if the Reynolds number increases, the friction coefficient decreases and has lower values than in spheres. Both the Reynolds number used and the droplet aspect ratio depend on the cross-sectional diameter of the droplet under study.

Research on liquid jet atomization in fuel droplets shows that a variety of models have been developed. These are generally focused on the determination of the droplet diameter, the jet penetration length, the angle of the envelope flare, the duration of the vaporisation process.

The models studied in the literature for multipoint injection systems rarely take into account the influence of the temperature of the gaseous medium in which the fuel spray occurs. The phenomenon of thermal diffusion is not taken into account when studying the evolution of the droplet diameter as it moves through a gaseous medium. The simulations have led to satisfactory results both quantitatively and qualitatively.

6. References

1. [Taylor,1964] Taylor, T., Acrivos, A., „On the deformation and drag of a falling drop at low Reynolds numbers”, J. Fluid Mech., Vol. 18, pp. 466–476, 1964.
2. [Philipp,2014] Philipp P., „Modeling of Collisional Transport Processes in Spray Dynamics”, Dissertation, RWTH Aachen University, pp.174, 2014.
3. [Bertakis,2010] Bertakis E., Groß S., Grande J., Fortmeier O., Reusken A., Pfennig A., „Validated simulation of droplet sedimentation with finite-element and level-set methods”, Chemical Engineering Science, No. 65, pp. 2037–2051, 2010.
4. [Clift,1978] Clift R., Grace J.R., Weber M.E., [Bubbles, Drops and Particles], New York & London, Academic Press, 383 pag., 1978.
5. [Beniuga,2015] Beniuga, M., Mihai, I., Suciu, C., Sprinceană, S., “Friction coefficient influence upon fluid jet atomization”, SPIE 9258, Advanced Topics in Optoelectronics, Microelectronics, and Nanotechnologies VII, Proc. 92582Q, doi: 10.1117/12.2070430, pp. 92582Q-1÷92582Q-6., 2015.
6. [Chryssakis,2005] Chryssakis C. A., Assanis D. N., [A Secondary Atomization Model for Liquid Droplet Deformation and Breakup under High Weber Number Conditions], ILASS Americas, 18th Annual Conference on Liquid Atomization and Spray Systems, Irvine, CA, pp. 1-8, 2005.
7. Mathcad 14, Licensed to: Stefan cel Mare University, Partially Product Code JE140709XX2311-XXD9-7VXX.